High-Resolution, Single-Molecule Measurements of Biomolecular Motion

William J. Greenleaf,[1] Michael T. Woodside,[3,4] and Steven M. Block[1,2]

[1]Department of Applied Physics and [2]Department of Biological Sciences, Stanford University, Stanford, California 94305–5030; email: sblock@stanford.edu

[3]National Institute for Nanotechnology, National Research Council of Canada, Edmonton AB, T6G 2V4, Canada

[4]Department of Physics, University of Alberta, Edmonton, AB, T6G 2G7, Canada

Annu. Rev. Biophys. Biomol. Struct. 2007. 36:171–90

First published online as a Review in Advance on February 28, 2007

The *Annual Review of Biophysics and Biomolecular Structure* is online at biophys.annualreviews.org

This article's doi: 10.1146/annurev.biophys.36.101106.101451

1056-8700/07/0609-0171$20.00

Key Words

optical trap, fluorescence, AFM, force clamp, magnetic tweezers

Abstract

Many biologically important macromolecules undergo motions that are essential to their function. Biophysical techniques can now resolve the motions of single molecules down to the nanometer scale or even below, providing new insights into the mechanisms that drive molecular movements. This review outlines the principal approaches that have been used for high-resolution measurements of single-molecule motion, including centroid tracking, fluorescence resonance energy transfer, magnetic tweezers, atomic force microscopy, and optical traps. For each technique, the principles of operation are outlined, the capabilities and typical applications are examined, and various practical issues for implementation are considered. Extensions to these methods are also discussed, with an eye toward future application to outstanding biological problems.

Contents

INTRODUCTION

Motor protein: a macromolecule that converts chemical energy (e.g., from NTP hydrolysis or proton motive force) into mechanical motion

F_1-ATPase: the component of the F_1F_0 ATP synthase that reversibly synthesizes ATP from ADP using a proton motive force

Flagellar motor: the molecular motor complex responsible for the rotation of flagella in motile bacteria and archaea

RNA polymerase (RNAP): a DNA-directed polymerase responsible for RNA transcription

Motion is fundamental to life. For centuries, the investigation of biological systems has involved the study of motion, from Antonie van Leeuwenhoek's (98) early observations of "living animalcules, very prettily a-moving" to contemporary measurements of single kinesin molecules walking along microtubules (95). Steady improvements in biophysical instrumentation over the past decades have enabled the detection of biomolecular motions in vitro with near-atomic resolution, allowing the mechanisms governing motion in a wide range of biological systems to be investigated at the level of single molecules and individual catalytic turnovers. Some of these studies have investigated classical mechanoenzymes, also called motor proteins, such as kinesin, dynein, and myosin (3, 30, 57, 95, 112); rotary motors like F_1-ATPase and the bacterial flagellar motor (67, 90); processive nucleic acid enzymes like RNA polymerase (RNAP), DNAP, λ-exonuclease, and RecBCD (51, 70, 71, 73, 78, 105, 113, 114); and topoisomerases (34, 66, 92). Other measurements have probed vesicle trafficking (5) and membrane fusion (11). A large number of single-molecule studies have also probed conformational changes in macromolecules, such as the folding and strain response of RNA, DNA, proteins, and polysaccharides (25, 33, 39, 50, 53, 55, 58, 84, 87, 103, 116).

The broad application of single-molecule methods to study molecular motions reflects the ability of these techniques to address a variety of biologically important questions. The simplest of these include measurements of the fundamental step sizes of motors (1, 26, 37, 95, 108), issues related to motor processivity and load-bearing ability (3, 86, 94, 114), and the kinetics and thermodynamics of mechanical response and folding transitions (29, 55, 69, 104). However, deeper questions about the mechanism of molecular motion can also be addressed by single-molecule methods. These include the coupling between chemical and mechanical cycles (1, 20, 80), mechanisms of translocation (4, 26, 44, 110, 112), folding pathways and the properties of transition states (29, 55, 69, 104), and issues of enzyme stochasticity and population heterogeneity (27, 96, 106).

This review discusses the principles, capabilities, and practical implementation of five of the most widely used methods for making high-resolution measurements of the motion of single molecules: particle tracking, fluorescence resonance energy transfer (FRET), magnetic tweezers, force-mode atomic force microscopy (AFM), and optical traps. These methods can be divided into two broad classes. Centroid tracking and FRET fall into a class of techniques that passively track the motion of labeled molecules without applying significant external force. Magnetic tweezers, AFM, and optical traps fall into a second class of techniques that measure motion under the application of an external mechanical load.

All single-molecule methods rely on the attachment of labels to the molecule of interest, which either scatter light (such as micron-sized beads) or emit it (such as fluorophores or quantum dots), to allow visualization of molecular motions. For force-based

methods, these labels must be attached to the molecule sufficiently well to withstand the forces being applied. Motion-reporter labels can be attached by using specific covalent interactions, specific noncovalent interactions, or nonspecific interactions. Covalent attachments based on amine-, thiol-, or carboxyl-reactive chemistries (41) can support large forces, on the order of 1 nN, but often involve harsh chemical treatments. Noncovalent attachments based, for example, on biotin-avidin (7), epitopes and antibodies, or metal chelation (79) are for this reason sometimes preferred. They can support forces from ~10 to ~300 pN (118). Nonspecific attachments such as pressure-induced (74) or charge-mediated (95) adsorption are simple to implement and can produce strong bonds, but the generally unknown orientation and mechanism of attachment can place limits on their application. For reasons of convenience or necessity, many single-molecule techniques have developed canonical linking chemistries, which may restrict their broader application to other specific systems of interest.

Aside from differences in the requirements of attachment chemistry, many of these techniques also operate in different regimes of spatial and temporal resolution, and they involve diverse levels of complexity in terms of the instrumentation required. Ideally, all of these characteristics should be matched to the requirements of a target biological system when choosing a particular experimental approach. A summary of features of the various methods is found **Table 1** and discussed in greater detail below.

PASSIVE SINGLE-MOLECULE METHODS

Centroid Tracking

The most straightforward and direct method for measuring molecular motion is to tag the molecule with a label that is easily visualized, such as a small reporter particle or a fluorescent dye molecule, and then use this label to track motion directly in an optical microscope (**Figure 1**).

Reporter particles. Some of the earliest measurements of biomolecular motion were carried out using microscopic beads attached to the molecule (32, 83), and this approach remains popular and effective (**Figure 1*a***). Reporter particles as diverse as micron-sized plastic or glass beads, gold particles, fluorescent beads, and fluorescent actin filaments or microtubules have all been used as suitable markers. These particles may be imaged with a microscope by using a variety of modalities, including brightfield, epifluorescence, differential interference contrast, back-focal-plane detection, or laser dark-field microscopy. The position of a molecule is inferred by tracking precisely the geometrical centroid (i.e., optical center of mass) of the particle image. The size, contrast range, and number of pixels in the imaging system determine the spatial resolution that can be achieved; typically, a digitized image allows the centroid to be located to within 1–2 nm (32), or about one tenth to one twentieth of a pixel, depending on the magnification. The temporal resolution is normally set by the image capture rate, but a fundamental limit is imposed by the characteristic relaxation time of the particle moving in its viscous medium.

Centroid tracking of particles is particularly well-suited to high-resolution measurements of rotary motion, as demonstrated by recent work on the dynamics of the F_1-ATPase and the bacterial flagellar motor. The F_1-ATPase is a part of the enzyme responsible for converting electrochemical potential into ATP; it can act as a rotary motor, producing torque through ATP hydrolysis. By attaching a fluorescently labeled, ~1-μm-long actin filament to the rotationally driven γ-subunit of F_1-ATPase, Kinosita and coworkers (67, 108) observed ATP-dependent rotation in discrete, 120° steps, confirming the Boyer model of ATP synthesis (12). Subsequent work increased the measurement bandwidth by replacing the long actin filaments

FRET: fluorescence resonant energy transfer

AFM: atomic force microscopy

Table 1 A comparison of high-resolution, single-molecule measurement techniques

	Optical traps	Magnetic tweezers	AFM	Centroid tracking: particle-based	Centroid tracking: single-molecule fluorescence based	FRET
Length scale probed	0.1–1000 nm	10–10,000 nm	1–10,000 nm	1–10,000 nm	1–10,000 nm	1–10 nm
Measurement timescale	10^{-4}–10^{3} s	10^{-3}–10^{5} s	10^{-3}–10^{2} s	10^{-2}–10^{2} s	10^{-1}–10^{2} s	10^{-3}–10^{2} s
Typical force range	0.1–100 pN	0.05–20 pN	5–10,000 pN	Nominally 0 pN; up to ~10 pN with drag	0 pN	0 pN
Reported spatial resolution	0.1 nm in 1-s window	10 nm in 1-s window	0.5 nm in 1-s window	1 nm in a 1-s window	1 nm per image	~1 nm, but difficult to calibrate
Typical attachment chemistries	Covalent, or specific noncovalent	Covalent, or specific noncovalent	Nonspecific	Noncovalent, or nonspecific	Covalent	Covalent
Additional capabilities	Active or passive force clamp Well-defined geometries	Constant force Applies torque or force	Can probe covalent bonds Active force clamp	Probe zero force Combine with flow control techniques Parallel measurements	Probe zero force	Ensemble measurements Detect internal motions Detect rotational conformations
Limitations	Photo-damage Bulky handles	Bulky handles Large particles Difficult to manipulate molecule	Polyproteins or chimeric constructs Random attachment geometries High-stiffness probe	Perturbation from large reporter particles	Limited dye lifetime (bleaching)	Dye bleaching, blinking, orientation dependence Crystal structure useful for interpretation

with 40-nm gold particles measured by laser dark-field microscopy, reducing the viscous drag on the label. These improvements revealed substeps in the motion of F_1-ATPase: The 120° catalytic cycle consisted of a 90° step associated with ATP binding and a subsequent 30° step associated with hydrolysis product release (109). These particle-tracking investigations have provided impressive insights into the mechanisms of biomechanical coupling in the F_1-ATPase, as well as direct measures of its performance as a molecular motor.

The bacterial flagellar motor is another complex machine driven by ion gradients across a membrane. It is employed by bacteria to generate motility and can rotate flagella at speeds of hundreds of hertz (56). Berry and coworkers (77, 90) observed that the motor takes 26 equal steps per rotation by attaching 200-nm fluorescent or 500-nm nonfluorescent polystyrene beads to individual flagella and monitoring rotational motion at up to 40 Hz using epifluorescence or back-focal-plane detection, respectively. This work addressed a longstanding problem by implicating the FliG protein ring, a structural component of the flagellar motor with the same 26-unit periodicity, as the component responsible for torque generation.

These examples illustrate some of the practical considerations involved in particle tracking to measure motion. In particular, particle size has a pronounced effect on the measurement, because larger particles, although easier to visualize, limit the temporal resolution through hydrodynamic drag, which introduces damping. In addition to limiting the temporal resolution, drag on particles also applies forces to the molecules under study. This effect may be turned to advantage by varying the particle size to load the motor differentially, allowing force-velocity characteristics to be measured (67).

Fluorescent dyes. When the perturbation induced by a reporter particle is too large, an effective alternative is to replace the particle with one or more fluorescent dyes attached to specific locations on the molecule and to visualize molecular motion by measuring the light emitted by the fluorophores (**Figure 1*b***). By fitting the intensity profile of the fluorophores to the appropriate point spread function (e.g., an Airy function or Gaussian), the centroid can be determined with an uncertainty, δx, of $\delta x = \sigma/\sqrt{N}$, where N is the number of photons counted and $\sigma \approx \lambda/(2NA)$ is the diffraction-limited spot size (λ is the wavelength of the emitted light and NA is the numerical aperture of the measurement system). The resolution of centroid tracking is thus not limited by the Rayleigh criterion, but rather by counting statistics at short timescales and, importantly, by any residual baseline drift or motion of the system at longer timescales.

Centroid tracking of single, fluorescently labeled molecules has recently been applied to study the stepping mechanism of classical molecular motors. By attaching a fluorophore to one head of the homodimeric motor protein myosin V, which moves in 37-nm steps (76), Selvin and coworkers (110) observed

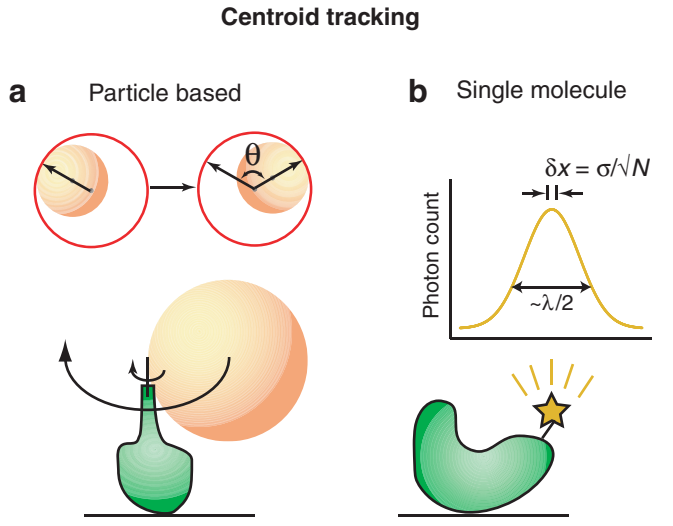

Figure 1

Centroid tracking of (*a*) particles and (*b*) single fluorescent molecules. Rotation can be monitored by measuring the motion of an attached, micron-sized particle. A single fluorophore attached to a protein of interest allows direct visualization of motion. By measuring the center of the fluorescence distribution, the fluorophore can be localized to ~1.5 nm.

directly that myosin V walks with a hand-over-hand mechanism, in which each head takes alternating steps of 74 nm. Similarly, by attaching a fluorophore to a single head of a dimeric kinesin molecule, which moves with 8-nm steps (95), Yildiz et al. (112) observed alternating 16-nm steps, helping to show that kinesin, too, moves by an alternating hand-over-hand mechanism.

Successful single-molecule fluorescence tracking requires attention to a number of complicating factors. Fluorophores must be attached covalently in a region where they will not disturb the function of the molecule and also will not be quenched, necessitating significant structural knowledge of the target molecule. Reactive oxygen species can also rapidly bleach fluorophores. To mitigate photobleaching, oxygen-scavenging systems are often used to extend fluorophore lifetime (111). Finally, methods to block out-of-focus fluorescence and minimize the sticking of fluorophores to the cover glass surface can significantly enhance the signal-to-noise ratio. Under ideal circumstances, using total internal reflection fluorescence microscopy and oxygen scavengers, this type of centroid tracking can determine the position of a tagged molecular motor to within 1.5 nm every second over an interval of ~1 min (hence it has been dubbed fluorescence imaging with one nanometer accuracy, or FIONA) (111).

Centroid tracking of single fluorophores reaches its limits, however, when trying to probe internal molecular rearrangements or small motions that occur on the millisecond timescale. Such motions, especially small conformational changes, are more typically studied with a different fluorescence-based technique: FRET.

Fluorescence Resonance Energy Transfer

FRET allows the measurement of nanometer-scale motions through the resonant coupling of two different fluorophores attached to the molecule of interest (38, 100). One of these fluorophores, the donor, is excited by external illumination. The donor then transfers energy nonradiatively via the Förster dipole-dipole interaction to a nearby acceptor fluorophore whose absorption spectrum overlaps the emission spectrum of the donor (**Figure 2**). The efficiency, *E*, of energy transfer varies as the sixth power of the donor-acceptor distance,

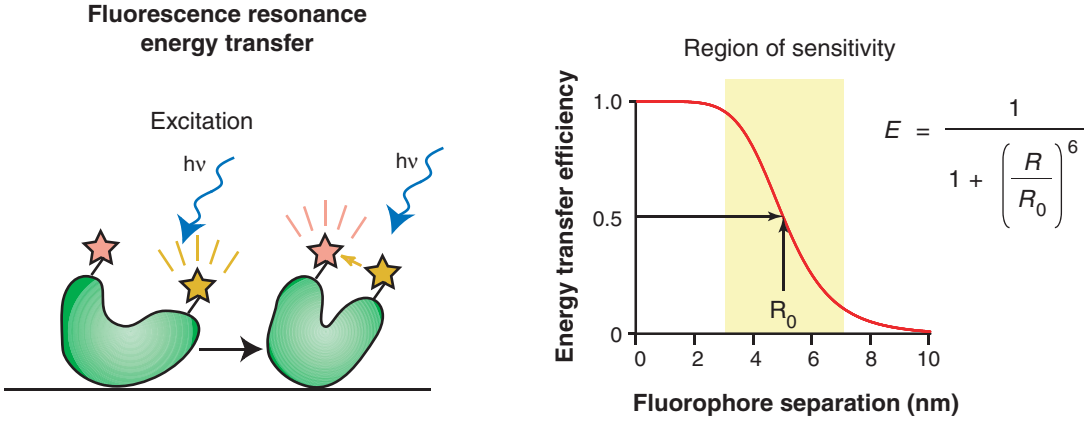

Figure 2

FRET mechanism and sensitivity. (*Left*) Excitation light (*blue*) excites the donor fluorophore (*yellow*). When the acceptor fluorophore (*red*) moves close to the excited donor, resonant energy transfer occurs, generating fluorescence centered at the acceptor wavelength (*red lines*). (*Right*) The efficiency of energy transfer is depicted with the region of sensitivity highlighted.

R: $E = 1/(1 + [R/R_0]^6)$, where the characteristic distance scale is given by the Förster radius R_0. Typical values for R_0 range from 2 to 6 nm (60), allowing displacements in the range of 1–10 nm to be observed. As the molecular conformation changes and the labeled portions of the molecule move with respect to one another, the FRET efficiency changes. Converting FRET efficiency into quantitative distances is difficult, however, because R_0 depends on the relative orientations of the fluorophores (38). For this reason, distances derived from FRET measurements are often interpreted qualitatively, or the FRET efficiencies are preassigned to specific molecular conformations in advance with the aid of other techniques.

Single-molecule FRET has been used to follow conformational changes in a wide variety of contexts, including the effects of calcium binding on calmodulin domains (13), the folding pathway of a cold-shock protein (81), the migration of Holliday junctions (59), the folding of telomeres (52), and transcription initiation (43). It has also been applied extensively to study the folding dynamics of single RNA molecules (115). RNA is a remarkably versatile macromolecule, capable not only of information storage, but also complicated three-dimensional folding and various catalytic functions. Chu and coworkers (116) probed the folding and catalytic activity of the *Tetrahymena* ribozyme, formed from a self-splicing group I intron, by observing FRET between dye pairs placed at the 3′ and 5′ ends of ribozymes tethered to a glass surface. These measurements supplied new insights into intermediate states and folding pathways. Similar measurements on the hairpin ribozyme, one of the simplest of catalytic RNAs, revealed complex interactions between folding and catalytic activity (117) and large heterogeneity in the folding behavior associated with loops formed in the ribozyme (96).

A number of practical issues require special attention to optimize FRET measurements. First, the donor and acceptor fluorophores must be selected carefully, so that both their emission and absorption spectra are reasonably well separated, yet with significant spectral overlap for efficient energy transfer. Commonly used fluorophore pairs with the appropriate spectral characteristics include Cy5 and Cy3, Cy3 and fluorescein, Alexa 488 and Alexa 594, blue-shifted GFP and red-shifted GFP, and even quantum dots (13, 38, 42, 81, 115). Other photophysics may strongly affect measurements: for example, blinking of the acceptor dye can mimic the desired FRET signals (38), and dye photobleaching may limit the duration of the measurement. Fluorescent molecules tend to generate a finite, characteristic number of photons on average before bleaching, typically less than one million (e.g., $\sim 10^5$ for Cy5). In practice, the FRET efficiency can be measured to ~10% accuracy for every 100 photons, allowing $\sim 10^3$ independent measurements with a maximum temporal resolution, set by fluorescence saturation, of ~1 ms (38).

Hairpin: a segment of a single-stranded nucleic acid, such as DNA or RNA, with a self-complimentary sequence capable of folding back and annealing to itself to form a duplex region

Ribozyme: a catalytically active molecule of RNA

FORCE-BASED SINGLE-MOLECULE METHODS

The Effects of Force on Molecular Motion and Resolution

The application of force to single molecules provides two principal advantages when measuring molecular motions: It can increase the resolution of the measurement by increasing the stiffness of the molecule under study, and it can allow the energy landscape for motions to be probed and manipulated. The natural reaction coordinate for the energy landscape of molecular motion is position. An external force perturbs the landscape owing to the mechanical work required to move against the load. As a result, force changes the heights of energy maxima and minima and hence the kinetics of the motion (**Figure 3**). Energetically unfavorable points on the landscape can be stabilized, and other properties of the landscape, such as the heights and positions of any transition states, can be reconstructed (28, 55, 104). Just as the dependence of catalysis on

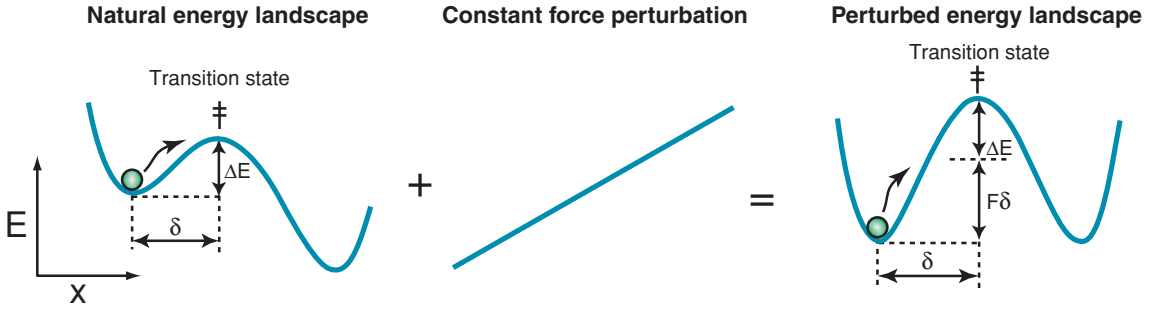

Figure 3

The effect of external force on the energy landscape. The natural energy landscape is altered by applying a constant force to produce a perturbed energy landscape. This perturbation changes the height of the energy barrier, ΔE, by an amount equal to Fδ.

substrate concentration reveals properties of substrate binding in a biochemical cycle, so too can the force dependence of motion reveal information about translocation steps in a chemomechanical cycle.

The increased measurement resolution that accompanies the application of force follows from the load-dependent stiffness, k, of molecular systems. Most molecules have nonlinear elastic compliance, and stiffness tends to increase with tension. Through the equipartition theorem, any increased stiffness reduces the thermal fluctuations in position that limit resolution according to $dx_{\mathrm{rms}} = \sqrt{k_B T/k}$, where k_B is the Boltzmann constant, T is the absolute temperature, and dx_{rms} is rms displacement. In practice, the resolution increase is enhanced because the motion of the molecule is sampled only at frequencies below the characteristic viscous damping frequency for the molecular motion, f_0. The power spectrum, S, of thermally driven positional motion in a harmonic potential is a Lorentzian:

$$S(f) = \frac{k_B T}{\pi^2 \beta (f_0^2 + f^2)},$$

where $f_0 = k/2\pi\beta$ is the roll-off frequency and β is the drag coefficient of the trapped particle. The mean-squared thermal displacement for a measurement band Δf below f_0 is then given by $\langle dx^2 \rangle = (4\beta k_B T \Delta f)/k^2$. Thermal fluctuations for a given measurement bandwidth can thus be reduced either by increasing the stiffness of the molecule (effectively reducing the amount of fluctuation) or by decreasing the drag coefficient β of the system (effectively moving fluctuations to higher frequencies where they become averaged by the measurement), as illustrated in **Figure 4**.

To apply force in a controlled way, the load must first be calibrated. One approach uses Brownian motion of the force probe itself (e.g., AFM cantilever, trapped microsphere) to determine its stiffness, k_{probe}, either through the equipartition theorem or through the roll-off frequency of the associated thermal power spectrum (93). Alternatively, the response of the probe to a known force, such as viscous drag from hydrodynamic flow, can be measured. These approaches all have characteristic systematic errors that can affect calibration (8).

The application of force using compliant force probes can introduce spurious effects, owing to the elasticity of the molecule-probe system (**Figure 5**). Often, molecular handles (e.g., DNA or polypeptides) are attached to the molecule under study in order to apply force in the desired way. These handles, the molecule of interest, and the force probe itself all act as compliant springs. As a result, a given motion of the molecule, δx_{mol}, will produce a correspondingly smaller probe motion, according to $\delta x_{\mathrm{probe}} = \delta x_{\mathrm{mol}} [k_{\mathrm{mol}}/(k_{\mathrm{mol}} + k_{\mathrm{probe}})]$, where the spring constants k_{mol} and k_{probe} refer to the molecular handle

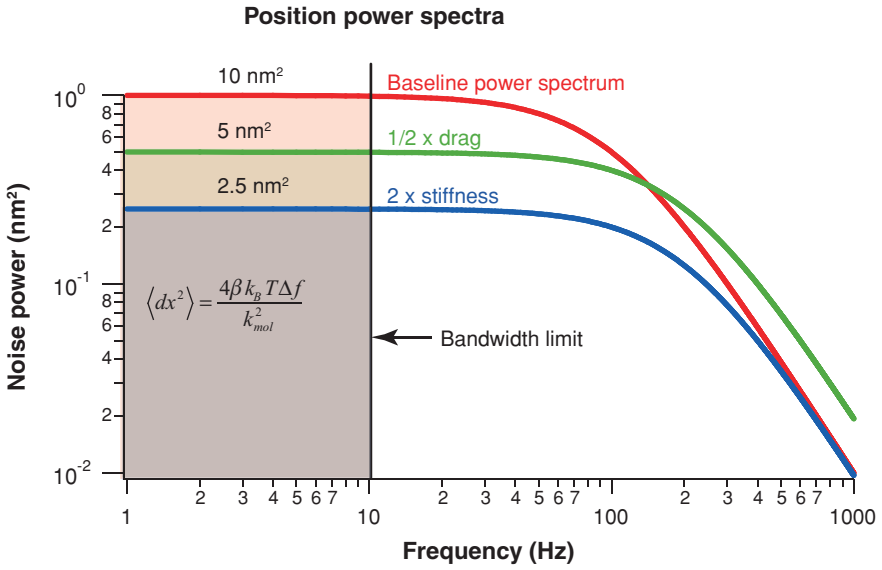

Figure 4

Brownian noise reduction in a limited bandwidth. Halving the viscous drag on the observed particle reduces mean-squared fluctuations in the measurement bandwidth by a factor of two. Stiffening the molecular handles by a factor of two reduces mean-squared fluctuations by a factor of four within this same region.

and probe, respectively. Moreover, motion of a spring-like probe necessarily changes the force applied to the molecule, complicating experimental interpretations. For these reasons, it is often convenient to employ a force clamp arrangement to maintain a constant load, either using active feedback (85) or passive methods (36). The use of a force clamp eliminates the need for compliance corrections due to changing system stiffnesses, and it can also improve the temporal resolution of displacement. However, force clamps using active feedback have a finite response time for engaging the feedback loop. This may complicate experimental interpretation if the response time, typically ~1–100 ms, is similar to the timescale for the motions being studied.

Magnetic Tweezers

Single molecules can be manipulated through magnetic forces by attaching them to small, superparamagnetic particles (**Figure 6**). These particles experience a force proportional to the magnetic field gradient, $F = \mu \nabla B$, where μ is the magnetic moment of the particle in a field B. The field gradient is usually treated as constant because the molecular motions are small compared with the length scale for changes in the field. Magnetic tweezers are thus intrinsically force-clamped, avoiding a need for active feedback methods. Lateral motions of the particle can be measured by centroid tracking, and axial motions can be tracked by imaging the height-dependent fringes arising in bright-field microscopy from interference between unscattered light and light scattered from the bead. These fringes can be calibrated precisely to resolve motions on the order of 10 nm (35). Force is calibrated by measuring the lateral Brownian motion of a bead tethered to the cover glass, e.g., by a long DNA molecule. The tether and bead form, in effect, an inverted pendulum driven by thermal energy and subject to a lateral restoring force $F\langle x \rangle / L$, where F is the magnetic force on the bead, $\langle x \rangle$ is

Force clamp: a device or method capable of maintaining a constant external load on an object, such as a macromolecule, as it moves

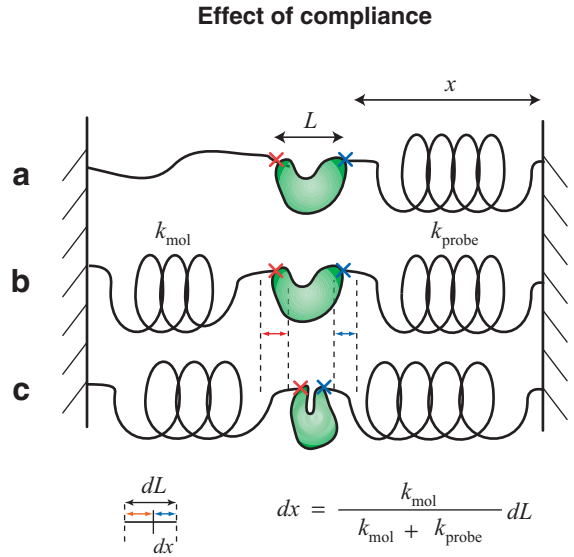

Figure 5

Measured distances are reduced by system compliance. (*a*) Force is applied by an elastic probe to a molecule (*green*) tethered by a molecular handle, and length changes are measured from the displacement of the force probe (*blue cross*). (*b*) The handle acts as a spring in series with the probe. (*c*) When molecular motion through a distance *dL* occurs, a portion of this displacement stretches the handle, reducing the observed displacement, *dx*, by an amount that depends on the relative stiffness of the molecule and the probe, as shown.

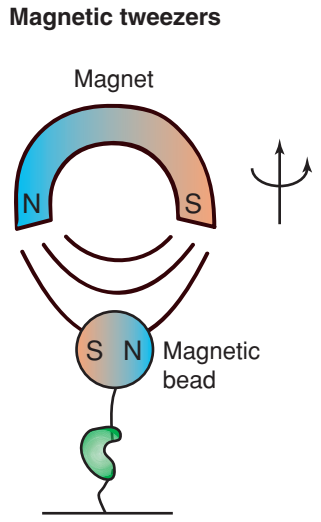

Figure 6

Magnetic tweezers. A superparamagnetic bead experiences a force in an inhomogeneous magnetic field and thereby applies load to a single molecule attached to its surface.

the lateral fluctuation, and L is the tether length. The magnetic force is found from the equipartition theorem, using $F = k_B TL/\langle x^2 \rangle$, or inferred in the time domain from the power spectrum of the Brownian motion (19). Magnetic tweezers can exert calibrated forces from as little as 0.05 pN up to ~20 pN, where the upper limit is set by the materials properties of the magnets and the dimensions of the paramagnetic beads (35).

In addition to applying force, magnetic tweezers can also apply torque, as magnetic beads act as dipoles with a preferred orientation in the magnetic field. Comparatively high torques (up to ~1000 pN nm^{-1}) can be applied to molecules attached to a bead in a torsionally constrained manner. To detect rotational motion, the spherical symmetry of the magnetic beads must be broken, which is often accomplished by manipulating small clusters of beads such that their angular orientation is clearly discernable by imaging (35). Such methods have been used to study the mechanical response of DNA to force and torque (33, 88, 91), the motion of the DNA translocase FtsK (10, 78), and the molecular mechanism of topoisomerases (47, 92). Recent work from Ebright and coworkers (73) also used magnetic tweezers to monitor the formation of a transcription bubble by RNAP with single-base precision through the generation of plectonemes in the DNA template. This experiment, along with single-molecule FRET studies (43), proved that transcription initiation involves scrunching of the DNA template. Magnetic tweezers typically have fairly limited temporal resolution mainly because of the viscous drag associated with the relatively large magnetic beads used (~1–4 μm in diameter). Although unmatched for producing torque (proportional to B), magnetic tweezers can apply only limited force (proportional to ∇B), and their axial and lateral position resolution is not as high as can be achieved with some of the other methods. However, they offer several advantages: Magnetic tweezers provide a stable platform for

measuring slow molecular processes involving both force and torque; they avoid completely the use of potentially damaging photon fluxes; they can harness the formation of plectonemes in DNA to amplify the motion of nucleic acid–based enzymes (19); and they involve relatively simple, straightforward instrumentation.

Atomic Force Microscopy

AFM uses a compliant cantilever to exert force upon a single molecule bound by one end to the cantilever probe tip and by its other end to a cover glass surface, which is typically moveable (**Figure 7**). The cantilever serves as a linear spring that develops a force $F = kx$, where k represents the cantilever stiffness and x represents the deflection. Cantilever stiffness may be calibrated from the power spectrum of thermal vibrations, and it is generally in the range of 10–100 pN nm^{-1} for single-molecule work. Cantilever deflection is typically monitored by a laser beam reflected from the probe onto a position-sensing detector (e.g., typical examples include quadrant photodiodes and position-sensitive diodes). Force can be modulated precisely by moving the surface with respect to the tip using piezoelectric actuators, thereby changing the cantilever deflection. Force may be clamped by moving this surface using position feedback in such a way that the deflection remains constant. The molecule under study is usually attached to the cantilever tip via nonspecific adsorption, by placing the tip in contact with the molecule and applying a large downbearing force (31). Such attachments can withstand 100–1000 pN of load but generally result in an unknown and uncontrolled attachment geometry.

AFM has been applied with success to study unfolding in a number of proteins, including ankyrin (50), spectrin (75), barnase (9), and GFP (25), as well as structural rearrangements in polysaccharides (58), by measuring changes in the extension of the molecules as these denature under external load. The most extensive investigations have been carried out for the protein titin, an enormous, filamentous molecule from muscle sarcomeres that carries multiple-tandem-repeat domains of several distinct types and is believed to furnish passive elasticity to muscle tissues. Several groups characterized the nanomechanical properties of single titin molecules, including the unfolding force and key features of the folding landscape (74, 102). They also compared their results to denaturant studies of unfolding (17) and reconstructed titin's role in muscle elasticity from single-molecule measurements of the individual structural components (53). The refolding of recombinant polyproteins, consisting of multiple repeats of a single protein domain of interest, has also been studied by Fernandez & Li (29), who found, for example, that polyubiquitin refolds in a complex energy landscape. Measurements on both

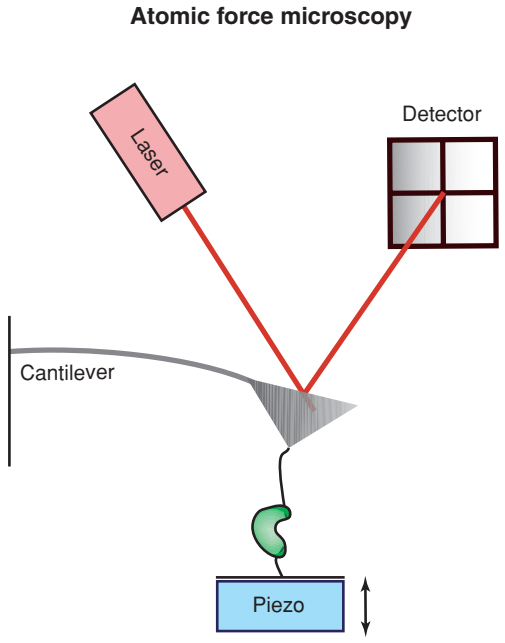

Figure 7

Atomic force microscopy. A cantilever exerts tension on a molecule of interest attached to the tip. Motions are measured by recording with a position-sensing detector the deflection of a laser beam reflected off the cantilever, and force is modulated by adjusting the position of the sample (or probe) piezoelectrically.

Position-sensing detector: a device that measures the average position of incident light

Titin: a protein that is a major constituent of vertebrate striated muscle and thought to guide the development of muscle thick filaments, as well as to provide passive elasticity in muscle fibers

polyubiquitin (15) and poly-GFP (24) also showed that the unfolding pathway depends on the location at which force is applied to the molecule.

Molecules with tandem repeats such as titin and polyprotein constructs are well suited for studies by AFM. Despite the random attachment points generated by the nonspecific binding to the probe, several repeats in series are generally placed under tension. The resulting regular array of characteristic sawtooth patterns observed in the force-extension curves, as each repeat unfolds, permits single molecules to be distinguished from multiple tethers or from various nonspecific interactions with the cover glass surface. Proteins that do not naturally have a tandem-repeat structure may be studied by forming recombinant chimeras between the proteins of interest and previously characterized, tandem-repeat handles (e.g., consisting of titin immunoglobulin-like domains or concatenated ubiquitin domains), which are then adsorbed nonspecifically to the tip (9). As a practical issue, care must be taken when designing single-molecule AFM studies to minimize potential complications arising from the nonspecific nature of the attachment to the AFM tip, the use of chimeric concatamers, and potentially complex interactions between the probe tip and the sample surface [via charge interactions, water exclusion, and other effects (118)].

Sources of noise affecting AFM measurements include motions of the sample with respect to the tip (e.g., acoustic coupling, thermal expansion, piezo creep) and optical interference effects between the tip and the surface. With careful isolation, instrument design, and alignment of the detection laser, such noise sources can be minimized, allowing intrinsic instrumental noise to be kept below the level of Brownian motion. However, because the tip of the cantilever is relatively large (hundreds of microns), viscous damping effects can limit detection bandwidth (see **Figure 4**). Because of the high cantilever stiffness, AFMs can be used to exert considerable force (between 10 and 10,000 pN), including forces sufficient to rupture covalent and high-affinity, noncovalent bonds. AFMs can therefore be used to measure the forces of ligand-substrate interactions for important macromolecular linkages, such as biotin-avidin, biotin-streptavidin, fluorescein/antifluorescein, and IgG/protein G (118), as well the unfolding forces of stable proteins (16) and the strength of disulfide bonds (101).

Optical Tweezers

Optical tweezers (or optical traps) employ a tightly focused laser beam to exert radiation pressure on a small dielectric bead to which one end of the molecule of interest is attached; the other end of the molecule is usually tethered to a surface or to a second bead (**Figure 8**). The strong electromagnetic field gradient near the focus polarizes the trapped bead, which experiences a force proportional to the gradient of the light intensity, according to $F = \alpha \nabla I_0$, where I_0 is the laser light intensity at the specimen and α is the bead polarizability (64). The force applied can be precisely modulated either by adjusting the intensity of the laser light or by altering the position of the bead with respect to the trap center (moving either the trap or the surface to which the molecule is attached), allowing the force exerted on the molecule to be clamped using a feedback loop. To minimize damage to molecules from the intense light associated with optical traps, the wavelengths used for optical trapping are generally chosen to be in the near infrared, which is a region of near-transparency for most biological materials (65), and catalytic systems are often employed for scavenging photoreactive species such as oxygen.

The position of the bead can be tracked by collecting the laser light scattered by the bead, either from the trapping laser itself or from a separate detection laser, using techniques such as optical trapping interferometry (23), back-focal-plane detection (99), or other variations

(87). Trap stiffness is calibrated either from the variance or the frequency spectrum of the Brownian motion of trapped beads or from the response of a trapped bead to viscous drag forces induced by fluid flow (93). Stiffnesses are typically lower than those for AFM cantilevers, generally 0.01–1 pN nm^{-1}, and consequently the forces that can be applied are also lower, generally 0.1–100 pN.

Optical tweezers have been applied to study a wide range of biophysical problems. The characteristics and mechanisms of the motion of classical mechanoenzymes such as kinesin (4, 44, 80, 94, 95), myosin (3, 30, 62, 76), and dynein (37, 57, 97) have been investigated in depth. Optical traps have also been used to probe the motion and mechanisms of processive nucleic acid enzymes such as exonucleases and helicases (26, 70, 71), DNA translocases (72) and polymerases (105), and RNAP (1, 2, 21, 40, 63, 82). In beautiful studies of the packaging of viral DNA into the phi29 bacteriophage, Bustamante and coworkers demonstrated that the rotary portal motor of the bacteriophage can package DNA against high forces (86), and elucidated a minimal kinetic model of force generation (20). Looking at RNAP, Block and coworkers studied the frequent pauses during transcription elongation (63), finding that they were off-pathway and sequence dependent (40) but unrelated to secondary structure in the RNA transcript (21). High-resolution measurements of the motion revealed single base-pair steps spanning 3.4 Å and provided significant constraints on possible models of chemomechanical coupling (1).

Optical tweezers have also been used to investigate the elastic properties of nucleic acids (84, 87), to study nonequilibrium kinetics (54), to measure protein-DNA interactions (46), and to characterize the folding of nucleic acids (55, 69, 104) and proteins (18, 45). By measuring the force-induced folding and unfolding of a single nucleic acid hairpin with very high position resolution and stability, Woodside et al. (103) determined the shape of the folding energy landscape along the full length of the reaction coordinate and identified the effects of sequence changes.

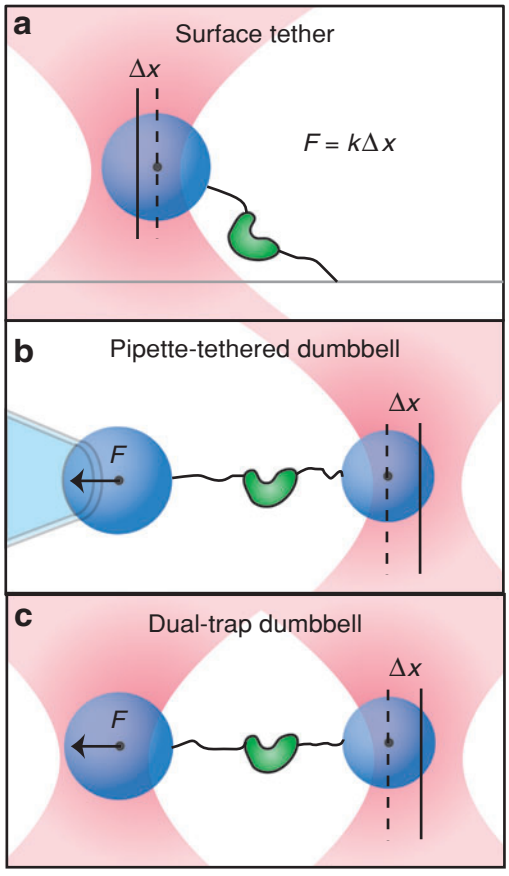

Figure 8

Comparison of the (*a*) surface-based assay, (*b*) dumbbell-based assay using one optical trap and a micropipette, and (*c*) dumbbell-based assay using two optical traps. Force is recorded by measuring the displacement of the bead from the center of the optical trap using light scattered by the bead.

When measuring motion with optical tweezers, the main instrumental consideration is the geometry to be used, which depends on both the system under study and the required resolution and stability. Surface-based assays, in which one end of the molecule is tethered to the trapped bead and the other end to the surface of a cover glass (**Figure 8*a***), are the simplest. However, they are susceptible to relative drift of the surface and the trap (e.g., due to thermal heating of the objective,

stage settling, laser pointing fluctuations, or acoustic noise coupling). By independently measuring the relative positions of the trap and surface, noise from surface drift can be reduced to ~1 Å (68). The pipette-tethered dumbbell assay (87), which involves attaching one end of the molecule to a bead held in the optical tweezers and the other to a bead held by a micropipette (**Figure 8*b***), allows for versatile manipulation of the sample and increased position sensitivity. This geometry, however, is still subject to the same noise sources as the surface-based assay, because of the mechanical connection through the micropipette.

Using a second optical trap instead of the micropipette (**Figure 8*c***) greatly reduces the mechanical noise, providing the most stable configuration (82). At this level, fluctuations in the relative positions of the laser beams induced by air currents contribute significantly to low-frequency noise. This noise can be suppressed by propagating the lasers through a gas with a low index of refraction, such as He ($n = 1.000035$) (1), or by careful isolation of the beam paths (61). The dual-trap dumbbell geometry also permits the simple implementation of an all-optical, passive force clamp to maintain constant force during the course of molecular motion, avoiding the complexities arising from finite-loop response times (36). Geometries with more than two traps are also possible (22).

With various improvements, optical traps have recently attained a resolution of 1 Å or better (at ~50 Hz) for the displacement of a trapped, micron-scale bead, which corresponds to determining position within the diameter of a single hydrogen atom. Dual-trap, independent-detector optical tweezers are complex instruments to produce, requiring at least three independent, diffraction-limited laser beams, some mechanism to control precisely the position of at least one trap at high bandwidth, and a low-vibration, temperature-stabilized environment for the apparatus. These devices can exert a large range of forces on small beads and have superior noise characteristics, but the required experimental geometry may be challenging to achieve in practice. Despite such limitations, optical traps are currently capable of measuring the motions of single biomolecules in real time over comparatively long timescales (minutes to hours) with atomic-level precision, which rivals the resolution attained by crystallographic methods.

FURTHER APPLICATIONS

Novel approaches to precision measurements of single-molecule motion continue to be developed. These new techniques include optical torque wrenches, which extend the functionality of optical tweezers to apply and measure controlled torque as well as force; various molecular rulers, which provide the means to measure motions and conformational changes on length scales both larger and smaller than those accessible by FRET; and combinations of force- and fluorescence-based techniques, which allow motions under load to be correlated with conformational changes.

An optical torque wrench (48) operates by trapping particles that are optically birefringent, i.e., possess either an anisotropic refractive index or a pronounced shape anisotropy. Such particles have a strong trapping axis, corresponding either to the slow optical axis or the long axis of the particle, which tends to align with the polarization of a linearly polarized trap beam. Rotation of the trap polarization exerts a torque on the particle as it attempts to maintain alignment with the polarization. The torque can be kept constant with a torque clamp, analogous to a force clamp, and the applied torque can be measured by detecting the change in angular momentum of the light scattered by the trapped particle. Torque wrenches should prove useful in studying systems with both rotary and linear components to their motion.

A number of spectroscopic molecular rulers are being developed to complement the capabilities of FRET. Single-molecule

electron transfer (107), in which distance-dependent electron transfer to a fluorophore modifies the fluorescence lifetime, is capable of measuring distance changes in the ångström and sub-ångström regimes. Distances at the 1- to 3-nm length scale have been measured using single-molecule optical switching (6), in which the recovery kinetics of a single Cy5 fluorophore switched into a dark state by an applied laser beam depends upon the spatial proximity of a Cy3 fluorophore. At the other end of the distance scale, motions at a distance of up to 70 nm can be monitored with 1 nm resolution, by measuring shifts in the plasmon resonance frequency of metallic nanoparticle probes (89). This method also avoids the problem of photobleaching, but at the cost of using large probes.

Combinations of different single-molecule techniques promise to provide powerful tools that bring to bear simultaneously the advantages of individual techniques. One example is the combination of fluorescence and optical trapping (49), which would be useful to probe directly questions regarding the coupling of mechanical and chemical steps in enzymatic reactions. Such combinations may be improved by design changes that compromise the performance of the constituent techniques but ensure the success of the whole, such as the use of chopped trapping and excitation beams in a combined fluorescence/trapping apparatus to improve signal-to-noise ratios and increase fluorescence lifetimes (14).

CONCLUSIONS

The high-resolution methods of single-molecule investigation described here provide a rich toolbox of precision probes suitable for the study of a wide range of interesting biomolecular motions. Given a particular system of interest, selecting the most appropriate single-molecule technique involves several considerations. Among these are the temporal and spatial resolution needed to resolve any relevant molecular motions, the desirability of applying either force or torque to the molecule, the variety of alternative methods available for the attachment of chemical labels or mechanical handles in a way that preserves function, and an assessment of the complexity and cost of any apparatus required, which must often be constructed, tested, and calibrated. The many successful applications of the various tools for studying single-molecule motion inspire hope that other, less well-understood instances of motion, that most fundamental characteristic of life, are ripe for future investigation.

LITERATURE CITED

1. Abbondanzieri EA, Greenleaf WJ, Shaevitz JW, Landick R, Block SM. 2005. Direct observation of base-pair stepping by RNA polymerase. *Nature* 438:460–65
2. Adelman K, La Porta A, Santangelo TJ, Lis JT, Roberts JW, Wang MD. 2002. Single molecule analysis of RNA polymerase elongation reveals uniform kinetic behavior. *Proc. Natl. Acad. Sci. USA* 99:13538–43
3. Altman D, Sweeney HL, Spudich JA. 2004. The mechanism of myosin VI translocation and its load-induced anchoring. *Cell* 116:737–49
4. Asbury CL, Fehr AN, Block SM. 2003. Kinesin moves by an asymmetric hand-over-hand mechanism. *Science* 302:2130–34
5. Babcock HP, Chen C, Zhuang XW. 2004. Using single-particle tracking to study nuclear trafficking of viral genes. *Biophys. J.* 87:2749–58
6. Bates M, Blosser TR, Zhuang X. 2005. Short-range spectroscopic ruler based on a single-molecule optical switch. *Phys. Rev. Lett.* 94:108101
7. Bayer EA, Wilchek M. 1980. The use of the avidin-biotin complex as a tool in molecular biology. *Methods Biochem. Anal.* 26:1–45

8. Berg-Sorensen K, Flyvbjerg H. 2004. Power spectrum analysis for optical tweezers. *Rev. Sci. Instrum.* 75:594–612
9. Best RB, Li B, Steward A, Daggett V, Clarke J. 2001. Can nonmechanical proteins withstand force? Stretching barnase by atomic force microscopy and molecular dynamics simulation. *Biophys. J.* 81:2344–56
10. Bigot S, Saleh OA, Cornet F, Allemand JF, Barre FX. 2006. Oriented loading of FtsK on KOPS. *Nat. Struct. Mol. Biol.* 13:1026–28
11. Bowen ME, Weninger K, Brunger AT, Chu S. 2004. Single molecule observation of liposome-bilayer fusion thermally induced by soluble N-ethyl maleimide sensitive-factor attachment protein receptors (SNAREs). *Biophys. J.* 87:3569–84
12. Boyer PD. 1993. The binding change mechanism for ATP synthase—some probabilities and possibilities. *Biochim. Biophys. Acta* 1140:215–50
13. Brasselet S, Peterman EJG, Miyawaki A, Moerner WE. 2000. Single-molecule fluorescence resonant energy transfer in calcium concentration dependent cameleon. *J. Phys. Chem. B* 104:3676–82
14. Brau RR, Tarsa PB, Ferrer JM, Lee P, Lang MJ. 2006. Interlaced optical force-fluorescence measurements for single molecule biophysics. *Biophys. J.* 91:1069–77
15. Carrion-Vazquez M, Li H, Lu H, Marszalek PE, Oberhauser AF, Fernandez JM. 2003. The mechanical stability of ubiquitin is linkage dependent. *Nat. Struct. Biol.* 10:674–76
16. Carrion-Vazquez M, Oberhauser AF, Fisher TE, Marszalek PE, Li HB, Fernandez JM. 2000. Mechanical design of proteins studied by single-molecule force spectroscopy and protein engineering. *Prog. Biophys. Mol. Biol.* 74:63–91
17. Carrion-Vazquez M, Oberhauser AF, Fowler SB, Marszalek PE, Broedel SE, et al. 1999. Mechanical and chemical unfolding of a single protein: a comparison. *Proc. Natl. Acad. Sci. USA* 96:3694–99
18. Cecconi C, Shank EA, Bustamante C, Marqusee S. 2005. Direct observation of the three-state folding of a single protein molecule. *Science* 309:2057–60
19. Charvin G, Allemand JF, Strick TR, Bensimon D, Croquette V. 2004. Twisting DNA: single molecule studies. *Contemp. Phys.* 45:383–403
20. Chemla YR, Aathavan K, Michaelis J, Grimes S, Jardine PJ, et al. 2005. Mechanism of force generation of a viral DNA packaging motor. *Cell* 122:683–92
21. Dalal RV, Larson MH, Neuman KC, Gelles J, Landick R, Block SM. 2006. Pulling on the nascent RNA during transcription does not alter kinetics of elongation or ubiquitous pausing. *Mol. Cell* 23:231–39
22. Dame RT, Noom MC, Wuite GJ. 2006. Bacterial chromatin organization by H-NS protein unravelled using dual DNA manipulation. *Nature* 444:387–90
23. Denk W, Webb WW. 1990. Optical measurement of picometer displacements of transparent microscopic objects. *Appl. Optics* 29:2382–91
24. Dietz H, Berkemeier F, Bertz M, Rief M. 2006. Anisotropic deformation response of single protein molecules. *Proc. Natl. Acad. Sci. USA* 103:12724–28
25. Dietz H, Rief M. 2004. Exploring the energy landscape of GFP by single-molecule mechanical experiments. *Proc. Natl. Acad. Sci. USA* 101:16192–97
26. Dumont S, Cheng W, Serebrov V, Beran RK, Tinoco I Jr, et al. 2006. RNA translocation and unwinding mechanism of HCV NS3 helicase and its coordination by ATP. *Nature* 439:105–8
27. English BP, Min W, van Oijen AM, Lee KT, Luo G, et al. 2006. Ever-fluctuating single enzyme molecules: Michaelis-Menten equation revisited. *Nat. Chem. Biol.* 2:87–94
28. Evans E, Ritchie K. 1997. Dynamic strength of molecular adhesion bonds. *Biophys. J.* 72:1541–55

29. Fernandez JM, Li HB. 2004. Force-clamp spectroscopy monitors the folding trajectory of a single protein. *Science* 303:1674–78
30. Finer JT, Simmons RM, Spudich JA. 1994. Single myosin molecule mechanics: piconewton forces and nanometre steps. *Nature* 368:113–19
31. Fisher TE, Marszalek PE, Fernandez JM. 2000. Stretching single molecules into novel conformations using the atomic force microscope. *Nat. Struct. Biol.* 7:719–24
32. Gelles J, Schnapp BJ, Sheetz MP. 1988. Tracking kinesin-driven movements with nanometre-scale precision. *Nature* 331:450–53
33. Gore J, Bryant Z, Nöllmann M, Le MU, Cozzarelli NR, Bustamante C. 2006. DNA overwinds when stretched. *Nature* 442:836–39
34. Gore J, Bryant Z, Stone MD, Nollmann MN, Cozzarelli NR, Bustamante C. 2006. Mechanochemical analysis of DNA gyrase using rotor bead tracking. *Nature* 439:100–4
35. Gosse C, Croquette V. 2002. Magnetic tweezers: micromanipulation and force measurement at the molecular level. *Biophys. J.* 82:3314–29
36. Greenleaf WJ, Woodside MT, Abbondanzieri EA, Block SM. 2005. Passive all-optical force clamp for high-resolution laser trapping. *Phys. Rev. Lett.* 95:208102
37. Gross SP, Welte MA, Block SM, Wieschaus EF. 2000. Dynein-mediated cargo transport in vivo. A switch controls travel distance. *J. Cell Biol.* 148:945–56
38. Ha T. 2001. Single-molecule fluorescence resonance energy transfer. *Methods* 25:78–86
39. Ha T, Zhuang XW, Kim HD, Orr JW, Williamson JR, Chu S. 1999. Ligand-induced conformational changes observed in single RNA molecules. *Proc. Natl. Acad. Sci. USA* 96:9077–82
40. Herbert KM, La Porta A, Wong BJ, Mooney RA, Neuman KC, et al. 2006. Sequence-resolved detection of pausing by single RNA polymerase molecules. *Cell* 125:1083–94
41. Hermanson GT. 1996. *Bioconjugate Techniques*. San Diego, CA: Academic
42. Hohng S, Ha T. 2005. Single-molecule quantum-dot fluorescence resonance energy transfer. *Chemphyschem* 6:956–60
43. Kapanidis AN, Margeat E, Ho SO, Kortkhonjia E, Weiss S, Ebright RH. 2006. Initial transcription by RNA polymerase proceeds through a DNA-scrunching mechanism. *Science* 314:1144–47
44. Kaseda K, Higuchi H, Hirose K. 2002. Coordination of kinesin's two heads studied with mutant heterodimers. *Proc. Natl. Acad. Sci. USA* 99:16058–63
45. Kellermayer MSZ, Smith SB, Granzier HL, Bustamante C. 1997. Folding-unfolding transitions in single titin molecules characterized with laser tweezers. *Science* 276:1112–16
46. Kotch SJ, Shundrovsky A, Jantzen BC, Wang MD. 2002. Probing protein-DNA interactions by unzipping a single DNA double helix. *Biophys J.* 83:1098–105
47. Koster DA, Croquette V, Dekker C, Shuman S, Dekker NH. 2005. Friction and torque govern the relaxation of DNA supercoils by eukaryotic topoisomerase IB. *Nature* 434:671–74
48. La Porta A, Wang MD. 2004. Optical torque wrench: angular trapping, rotation, and torque detection of quartz microparticles. *Phys. Rev. Lett.* 92:190801
49. Lang MJ, Fordyce PM, Engh AM, Neuman KC, Block SM. 2004. Simultaneous, coincident optical trapping and single-molecule fluorescence. *Nat. Methods* 1:133–39
50. Lee G, Abdi K, Jiang Y, Michaely P, Bennett V, Marszalek PE. 2006. Nanospring behavior of ankyrin repeats. *Nature* 440:246–49
51. Lee JB, Hite RK, Hamdan SM, Xie XS, Richardson CC, van Oijen AM. 2006. DNA primase acts as a molecular brake in DNA replication. *Nature* 439:621–24

52. Lee JY, Okumus B, Kim DS, Ha TJ. 2005. Extreme conformational diversity in human telomeric DNA. *Proc. Natl. Acad. Sci. USA* 102:18938–43
53. Li H, Linke WA, Oberhauser AF, Carrion-Vazquez M, Kerkvliet JG, et al. 2002. Reverse engineering of the giant muscle protein titin. *Nature* 418:998–1002
54. Liphardt J, Dumont S, Smith SB, Tinoco I Jr, Bustamante C. 2002. Equilibrium information from nonequilibrium measurements in an experimental test of Jarzynski's equality. *Science* 296:1832–35
55. Liphardt J, Onoa B, Smith SB, Tinoco I Jr, Bustamante C. 2001. Reversible unfolding of single RNA molecules by mechanical force. *Science* 292:733–36
56. Lowe G, Meister M, Berg HC. 1987. Rapid rotation of flagellar bundles in swimming bacteria. *Nature* 325:637–40
57. Mallik R, Carter BC, Lex SA, King SJ, Gross SP. 2004. Cytoplasmic dynein functions as a gear in response to load. *Nature* 427:649–52
58. Marszalek PE, Oberhauser AF, Pang YP, Fernandez JM. 1998. Polysaccharide elasticity governed by chair-boat transitions of the glucopyranose ring. *Nature* 396:661–64
59. McKinney SA, Freeman ADJ, Lilley DMJ, Ha TJ. 2005. Observing spontaneous branch migration of Holliday junctions one step at a time. *Proc. Natl. Acad. Sci. USA* 102:5715–20
60. Moerner WE, Fromm DP. 2003. Methods of single-molecule fluorescence spectroscopy and microscopy. *Rev. Sci. Instrum*. 74:3597–619
61. Moffitt JR, Chemla YR, Izhaky D, Bustamante C. 2006. Differential detection of dual traps improves the spatial resolution of optical tweezers. *Proc. Natl. Acad. Sci. USA* 103:9006–11
62. Molloy JE, Burns JE, Kendrick-Jones J, Tregear RT, White DC. 1995. Movement and force produced by a single myosin head. *Nature* 378:209–12
63. Neuman KC, Abbondanzieri EA, Landick R, Gelles J, Block SM. 2003. Ubiquitous transcriptional pausing is independent of RNA polymerase backtracking. *Cell* 115:437–47
64. Neuman KC, Block SM. 2004. Optical trapping. *Rev. Sci. Instrum*. 75:2787–809
65. Neuman KC, Chadd EH, Liou GF, Bergman K, Block SM. 1999. Characterization of photodamage to *Escherichia coli* in optical traps. *Biophys. J*. 77:2856–63
66. Neuman KC, Charvin G, Bensimon D, Croquette V. 2005. Single-molecule study of DNA unlinking by topoisomerase IV: influence of the crossing angle. *Biophys. J*. 88:15a
67. Noji H, Yasuda R, Yoshida M, Kinosita K. 1997. Direct observation of the rotation of F1-ATPase. *Nature* 386:299–302
68. Nugent-Glandorf L, Perkins TT. 2004. Measuring 0.1-nm motion in 1 ms in an optical microscope with differential back-focal-plane detection. *Optics Lett*. 29:2611–13
69. Onoa B, Dumont S, Liphardt J, Smith SB, Tinoco I Jr, Bustamante C. 2003. Identifying kinetic barriers to mechanical unfolding of the *T. thermophila* ribozyme. *Science* 299:1892–95
70. Perkins TT, Dalal RV, Mitsis PG, Block SM. 2003. Sequence-dependent pausing of single lambda exonuclease molecules. *Science* 301:1914–18
71. Perkins TT, Li HW, Dalal RV, Gelles J, Block SM. 2004. Forward and reverse motion of single RecBCD molecules on DNA. *Biophys. J*. 86:1640–48
72. Ptacin JL, Nollmann M, Bustamante C, Cozarelli NR. 2006. Identification of the FtsK sequence-recognition domain. *Nat. Struct. Mol. Biol*. 13:1023–25
73. Revyankin A, Liu C, Ebright RH, Strick TR. 2006. Abortive initiation and productive initiation by RNA polymerase involve DNA scrunching. *Science* 314:1139–43
74. Rief M, Gautel M, Oesterhelt F, Fernandez JM, Gaub HE. 1997. Reversible unfolding of individual titin immunoglobulin domains by AFM. *Science* 276:1109–12

75. Rief M, Pascual J, Saraste M, Gaub HE. 1999. Single molecule force spectroscopy of spectrin repeats: low unfolding forces in helix bundles. *J. Mol. Biol.* 286:553–61
76. Rock RS, Rice SE, Wells AL, Purcell TJ, Spudich JA, Sweeney HL. 2001. Myosin VI is a processive motor with a large step size. *Proc. Natl. Acad. Sci. USA* 98:13655–59
77. Rowe AD, Leake MC, Morgan H, Berry RM. 2003. Rapid rotation of micron and submicron dielectric particles measured using optical tweezers. *J. Modern Optics* 50:1539–54
78. Saleh OA, Perals C, Barre FX, Allemand JF. 2004. Fast, DNA-sequence independent translocation by FtsK in a single-molecule experiment. *EMBO J.* 23:2430–39
79. Schmitt L, Ludwig M, Gaub HE, Tampe R. 2000. A metal-chelating microscopy tip as a new toolbox for single-molecule experiments by atomic force microscopy. *Biophys. J.* 78:3275–85
80. Schnitzer MJ, Block SM. 1997. Kinesin hydrolyses one ATP per 8-nm step. *Nature* 388:386–90
81. Schuler B, Lipman EA, Eaton WA. 2002. Probing the free-energy surface for protein folding with single-molecule fluorescence spectroscopy. *Nature* 419:743–47
82. Shaevitz JW, Abbondanzieri EA, Landick R, Block SM. 2003. Backtracking by single RNA polymerase molecules observed at near-base-pair resolution. *Nature* 426:684–87
83. Sheetz MP, Turney S, Qian H, Elson EL. 1989. Nanometre-level analysis demonstrates that lipid flow does not drive membrane glycoprotein movements. *Nature* 340:284–88
84. Seol Y, Skinner GM, Visscher K. 2004. Elastic properties of a single-stranded charged homopolymeric ribonucleotide. *Phys. Rev. Lett.* 93:118102
85. Simmons RM, Finer JT, Chu S, Spudich JA. 1996. Quantitative measurements of force and displacement using an optical trap. *Biophys. J.* 70:1813–22
86. Smith DA, Tans SJ, Smith SB, Grimes S, Anderson DL, Bustamante C. 2001. The bacteriophage phi29 portal motor can package DNA against a large internal force. *Nature* 413:748–52
87. Smith SB, Cui Y, Bustamante C. 1996. Overstretching B-DNA: the elastic response of individual double-stranded and single-stranded DNA molecules. *Science* 271:795–99
88. Smith SB, Finzi L, Bustamante C. 1992. Direct mechanical measurements of the elasticity of single DNA molecules by using magnetic beads. *Science* 258: 1122–26
89. Sönnichsen C, Reinhard BM, Liphardt J, Alivisatos AP. 2005. A molecular ruler based on plasmon coupling of single gold and silver nanoparticles. *Nat. Biotechnol.* 23:741–45
90. Sowa Y, Rowe AD, Leake MC, Yakushi T, Homma M, et al. 2005. Direct observation of steps in rotation of the bacterial flagellar motor. *Nature* 437:916–19
91. Strick TR, Alleman JF, Bensimon D, Bensimon A, Croquette V. 1996. The elasticity of a single supercoiled DNA molecule. *Science* 271:1835–37
92. Strick TR, Croquette V, Bensimon D. 2000. Single-molecule analysis of DNA uncoiling by a type II topoisomerase. *Nature* 404:901–4
93. Svoboda K, Block SM. 1994. Biological applications of optical forces. *Annu. Rev. Biophys. Biomol. Struct.* 23:247–85
94. Svoboda K, Block SM. 1994. Force and velocity measured for single kinesin molecules. *Cell* 77:773–84
95. Svoboda K, Schmidt CF, Schnapp BJ, Block SM. 1993. Direct observation of kinesin stepping by optical trapping interferometry. *Nature* 365:721–27
96. Tan E, Wilson TJ, Nahas MK, Clegg RM, Lilley DMJ, Ha T. 2003. A four-way junction accelerates hairpin ribozyme folding via a discrete intermediate. *Proc. Natl. Acad. Sci. USA* 100:9308–13

97. Toba S, Watanabe TM, Yamaguchi-Okimo L, Toyoshima YY, Higuchi H. 2006. Overlapping hand-over-hand mechanism of single molecular motility of cytoplasmic dynein. *Proc. Natl. Acad. Sci. USA* 103:5741–45
98. van Leeuwenhoek A. 1683. *Letter to Francois Aston, Delft, 12 Sept 1683, p. 11*
99. Visscher K, Gross SP, Block SM. 1996. Construction of multiple-beam optical traps with nanometer-resolution position sensing. *IEEE J. Select. Top. Quant. Electron*. 2:1066–76
100. Weiss S. 2000. Measuring conformational dynamics of biomolecules by single molecule fluorescence spectroscopy. *Nat. Struct. Biol*. 7:724–29
101. Wiita AP, Ainavarapu SR, Huang HH, Fernandez JM. 2006. Force-dependent chemical kinetics of disulfide bond reduction observed with single-molecule techniques. *Proc. Natl. Acad. Sci. USA* 103:7222–27
102. Williams PM, Fowler SB, Best RB, Toca-Herrera JL, Scott KA, et al. 2003. Hidden complexity in the mechanical properties of titin. *Nature* 422:446–49
103. Woodside MT, Anthony PC, Behnke-Parks WM, Larizadeh K, Herschlag D, Block SM. 2006. Direct measurement of the full, sequence-dependent folding landscape of a nucleic acid. *Science* 314:1001–4
104. Woodside MT, Behnke-Parks WM, Larizadeh K, Travers K, Herschlag D, Block SM. 2006. Nanomechanical measurements of the sequence-dependent folding landscapes of single nucleic acid hairpins. *Proc. Natl. Acad. Sci. USA* 103:6190–95
105. Wuite GJ, Smith SB, Young M, Keller D, Bustamante C. 2000. Single-molecule studies of the effect of template tension on T7 DNA polymerase activity. *Nature* 404:103–6
106. Xie Z, Srividya N, Sosnick TR, Pan T, Scherer NF. 2004. Single-molecule studies highlight conformational heterogeneity in the early folding steps of a large ribozyme. *Proc. Natl. Acad. Sci. USA* 101:534–39
107. Yang H, Luo G, Karnchanaphanurach P, Louie T-M, Rech I, et al. 2003. Protein conformational dynamic probed by single-molecule electron transfer. *Science* 302:262–66
108. Yasuda R, Noji H, Kinosita KJ, Yoshida M. 1998. F1-ATPase is a highly efficient molecular motor that rotates with discrete 120° steps. *Cell* 93:1117–24
109. Yasuda R, Noji H, Yoshida M, Kinosita KJ, Itoh H. 2001. Resolution of distinct rotational substeps by submillisecond kinetic analysis of F1-ATPase. *Nature* 410:898–904
110. Yildiz A, Forkey JN, McKinney SA, Ha T, Goldman YE, Selvin PR. 2003. Myosin V walks hand-over-hand: single fluorophore imaging with 1.5-nm localization. *Science* 300:2061–65
111. Yildiz A, Selvin PR. 2005. Fluorescence imaging with one nanometer accuracy: application to molecular motors. *Acc. Chem. Res*. 38:574–82
112. Yildiz A, Tomishige M, Vale RD, Selvin PR. 2004. Kinesin walks hand-over-hand. *Science* 303:676–78
113. Yin H, Landick R, Gelles J. 1994. Tethered particle motion method for studying transcript elongation by a single RNA polymerase molecule. *Biophys. J*. 67:2468–78
114. Yin H, Wang MD, Svoboda K, Landick R, Block SM, Gelles J. 1995. Transcription against an applied force. *Science* 270:1653–57
115. Zhuang X. 2005. Single-molecule RNA science. *Annu. Rev. Biophys. Biomol. Struct*. 34:399–414
116. Zhuang X, Bartley LE, Babcock HP, Russell R, Ha T, et al. 2000. A single-molecule study of RNA catalysis and folding. *Science* 288:2048–51
117. Zhuang X, Kim H, Pereira MJ, Babcock HP, Walter NG, Chu S. 2002. Correlating structural dynamics and function in single ribozyme molecules. *Science* 296:1473–76
118. Zlatanova J, Lindsay SM, Leuba SH. 2000. Single molecule force spectroscopy in biology using the atomic force microscope. *Prog. Biophys. Mol. Biol*. 74:37–61

Annual Review of Biophysics and Biomolecular Structure

Volume 35, 2006

Contents